Droop Coefficient Design and Optimization Using Genetic Algorithm- A Case Study of the More Electric Aircraft DC Microgrid

Habibu Hussaini [1,2], Tao Yang [1*], Yuan Gao [1], Cheng Wang [1], Ge Bai [1], Serhiy Bozhko [1]
[1] Power Electronics, Machines and Control (PEMC) Research Group, Faculty of Engineering, University of Nottingham, Nottingham, NG7 2RD, UK
[2] Department of Electrical and Electronics Engineering, Federal University of Technology, PMB 065, Gidan-Kwanu Main Campus, Bida Road, Minna, Niger State, Nigeria
[*]Corresponding Author: Tao.Yang@nottingham.ac.uk

***Abstract*—The droop control method is usually employed in the DC microgrids to share the load current demand among multiple sources due to its advantage of being independent of a communication network. However, the performance of the droop control method is affected by the mismatched transmission line resistance and the offset in the nominal voltage reference. This paper presents the design and optimization of the droop coefficient of converters, using the genetic algorithm to enhance the current sharing and the DC bus voltage regulation performance. The proposed approach is tested on the single bus multi-source electrical power system (EPS) for the more electric aircraft (MEA) applications. The effectiveness of the proposed approach is validated using a detailed simulation model of the MEA EPS developed in MATLAB Simulink.**

Keywords—Design, droop coefficient, droop control, genetic algorithm, more electric aircraft, optimization

I. INTRODUCTION

The 270 V single bus multi-source electrical power system (EPS) configuration for the future more electric aircraft (MEA) distribution network is used as a case study in this paper. This system can be considered a typical DC microgrid (MG). The system is made up of multiple sources that are connected in parallel and interfaced to corresponding parallel-connected active rectifiers (AR_{1-3}) and linked to a common 270 V DC bus via transmission cables as shown in Fig. 1. The sources are usually permanent magnet synchronous generators (PMSGs). The transmission cable impedance in the DC MG is predominantly resistive. The auxiliary power unit (APU) is typically used to provide power to the aircraft in an emergency or when the aircraft is on the ground [1, 2, 3].

When multiple sources are connected in parallel, it helps to enhance the redundancy of the power system. However, issues of load sharing among the multiple sources and the DC bus voltage regulation are of great concern. Also, the proper control of the converters plays a key role in the management and control of the MG operation. The basic objective considered here is to realize an accurate current sharing among multiple sources and the DC bus voltage regulation. Different approaches such as the master-slave, centralized control, distributed control and droop control have been employed for the accurate power sharing among sources and regulation of the DC bus voltage, as reported in the literature [4, 5, 6]. However, the droop control method is the most widely employed for the DC MG. This is due to its advantage of being independent of a communication medium, high reliability, and modularity [6, 7].

In the traditional droop control method, the droop coefficients are usually selected to be fixed for each converter and are based on the converter's current ratings to achieve appropriate current sharing. Accurate sharing of the load

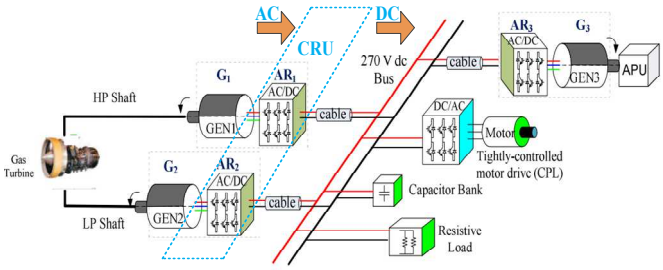

Fig. 1. 270 V Single bus EPS Architecture for future MEA application used as case study [3]

current demand will ensure that none of the sources is overloaded or thermally stressed [2]. However, the traditional droop control method with a fixed droop coefficient has limitations when the resistance of the lines is mismatched and there is a nominal voltage reference offset [2]. This is largely due to the unequal voltage drops across the transmission lines connecting the parallelled converters to the DC bus. Hence, this can lead to inaccurate current sharing and poor bus voltage regulation. It is important to mention that there is usually a need for a trade-off between current sharing accuracy and voltage regulation when using the droop control method with a fixed droop coefficient [8]. However, even with the existence of the trade-off, droop control is still a competitive solution for both small and large-scale DC MGs [9].

Several approaches have been proposed to enhance the performance of the droop control method, as reported in the literature [10, 11, 12, 13]. Some of these proposed methods can achieve appropriate power sharing with the aid of a communication network [12], the knowledge of the line resistance is required in [10] to adjust the droop coefficient of the converters, and the adaptive tuning of the droop coefficient based on the loading condition is another approach proposed in [13]. Some of these approaches may not be robust and reliable in ensuring optimal performance in the operation of the MG. Consequently, it is paramount to find a way of computing the optimal droop coefficient of the converters that will yield the desired control objectives.

In the recent decade, different intelligent algorithms have also been employed for the computation of the converter's optimal droop coefficients [14, 15, 16, 17, 18, 19]. For example, the particle swarm optimization is used for the optimization of the droop parameters in [14, 15, 16, 18] for a single bus DC MG system, the harmony search (HS) algorithm is utilized in [17] and the nondominated sorting genetic algorithm (NSGA II) is employed in [19] for the parallel and mesh connected MGs. The weighted sum technique is used in [14, 15] to convert the multiobjective optimization (MOO) to a single objective. However, this

requires the knowledge of the optimum weighting factor to obtain the best compromise solution. Hence, making the process complex. Also, the approach proposed in [19] requires the use of the fuzzy membership function to obtain the optimal design point. Furthermore, in these previous works, one of the objectives considered is the minimization of the error in the output DC currents while this paper studies the current sharing ratio for optimization.

Therefore, this paper aims to reduce the computational complexity and simplify the objective functions by (1) formulating the objective functions to be numbers between 0 and 1 and (2) eliminating the weighting factor in the objective formulation and the need to tune it. Thus, using objective normalization, it is hoped that the optimization process speed and accuracy will be improved. Moreover, computational algorithms tend to find it easier to manipulate numbers between 0 and 1 [20]. Also, a simple integrated objective function is used to extract the optimal design point from the Pareto front results. Furthermore, the studied system is the 270 V single DC bus MEA EPS distribution network which has not been considered in the previous works. Consequently, to enhance the performance of the droop control method, a procedure for the design, optimization and automated selection of the fixed droop coefficient of the power converters is proposed in this paper.

II. Analysis of the Droop Control Method

Fig. 2 shows the detailed control structure of the MEA EPS distribution network using the voltage-mode droop control scheme. Only one source and one converter are shown in Fig. 2 to conserve space. However, the control of three sources is considered in this paper. The detailed MEA EPS control model will be used as a case study in the proposed genetic algorithm-based droop coefficient design and optimization approach.

The steady-state equivalent circuit model of the MEA EPS distribution network is shown in Fig. 3. The parallel-connected sources with the interfaced converters shown in Fig. 1 are modelled as an ideal voltage source followed by a virtual resistance under the droop control method as shown in Fig. 3. Also, the transmission cable connecting the parallel-connected converters to the DC bus is modelled as resistance for the analysis of the steady-state operation.

The traditional droop control is realized by linearly decreasing the output DC voltage as the output current increases [21]. The output voltage reference of the droop controlled converter in Fig. 3 is as expressed in (1).

$$V_{dci}^{*} = V_{0i} - R_{di} I_{dci} \tag{1}$$

where the fixed virtual droop coefficient and the nominal voltage reference of the *i*th DC source under no-load conditions are represented by R_{di} and V_{0i} respectively. Under the no-load condition, $V_{01} = V_{02} = V_0$.

The value of the droop coefficient for each converter is usually limited and conventionally design based on the current ratings of the converters as expressed in (2).

$$R_{di} \leq \frac{\delta V_{max}}{I_{dcimax}} \tag{2}$$

where I_{dcimax} is the maximum/full-load output current of the *i*th converter and the maximum allowable deviation of the DC bus voltage is denoted as δV_{max}. This way the voltage deviation at the output of each of the converters due to the droop action is limited within the maximum tolerable value. The value of δV_{max} is usually set to be about 5% of the nominal voltage. However, the main DC bus nominal voltage and range are defined according to the MIL-STD-704F standard for the aircraft electrical power system and other electrical loads [22]. For the MEA EPS, 270 V is the nominal voltage and a range between 250 V and 280 V variation is acceptable in the steady-state.

Assuming the transmission cable impedance can be ignored, expression in (3) shows the current sharing ratio between the sources in steady-state.

$$I_{dc1} : I_{dc2} = \frac{1}{k_{d1}} : \frac{1}{k_{d2}} \tag{3}$$

where $k_{d1}=R_{d1}$ *and* $k_{d2}=R_{d2}$ are the droop coefficient of the converters.

It can be observed from (3) that droop coefficients are selected to be inversely proportional to the current ratings of the converters. This is to ensure that the droop controller can provide accurate current sharing among the sources if the same nominal voltage V_0 is applied to each of the droop characteristics and the transmission cable impedance can be neglected. However, the transmission cable impedance can only be neglected in a small system. In a large and low voltage DC MG, the transmission cable impedance cannot be ignored as it affects the performance of the droop controller. Moreover, the cable resistance cannot be ignored in a practical situation. The limitations of the conventional droop control method in achieving accurate current sharing and DC bus voltage regulation are discussed in detail as follows.

A. Degradation of the DC Bus Voltage

As expressed in (1), there is the existence of an unavoidable DC voltage deviation in the output of the converters due to the droop action. However, these deviations can be limited within a tolerable range by choosing an appropriate value of the droop coefficient of the converters based on the expression in (2). These deviations at the output voltage of the converters cause the degradation of the DC bus voltage. Additionally, coupled with the voltage drop across the line resistance, the DC bus voltage regulation becomes deteriorated. Hence, when the voltage drop on the cables is taken into consideration and the voltage control dynamics are ignored, the steady-state DC bus voltage is as expressed in (4).

$$V_b = V_{dci}^{*} - R_i I_{dci} = V_0 - (R_{di} + R_i) I_{dci} \tag{4}$$

where R_i is the resistance of the cables connecting the *i*th DC source to the load and V_b is the main DC bus voltage.

B. Degradation in the Current Sharing Accuracy

Similarly, when the line resistance is taken into consideration, the output DC voltage at the terminal of each of the converters will not be the same due to the unequal voltage drop across the unequal line resistance, hence, affecting the load current sharing accuracy. Therefore, based on the expression in (4), the current sharing ratio between the sources is as expressed in (5).

$$I_{dc1} : I_{dc2} = \frac{1}{k_{d1}+R_1} : \frac{1}{k_{d2}+R_2} \leftrightarrow \frac{I_{dc1}}{I_{dc2}} = \frac{k_{d2}+R_2}{k_{d1}+R_1} \tag{5}$$

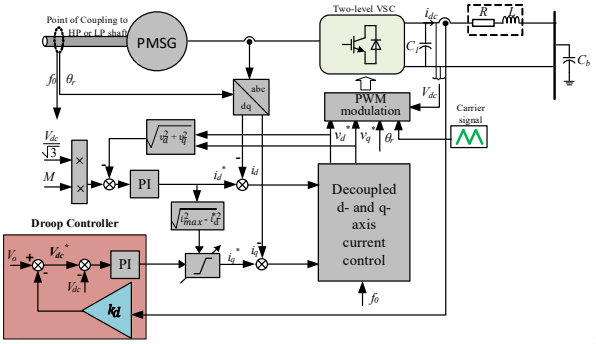

Fig. 2. Voltage-mode droop control scheme of a generator source fed by an active rectifier (AR) in the studied MEA EPS.

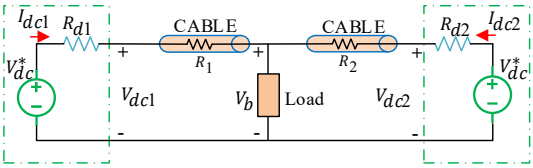

Fig. 3. Steady-state Equivalent Circuit of the Distribution Network

It can be observed from (5) that the current sharing ratio of the sources will be impacted by both the cable resistance and droop coefficient. To mitigate the influence of the line resistance on the current sharing performance of the droop controller, the value of the droop coefficient for each of the converters is selected to be larger than the corresponding line resistance (i.e. $k_{di} \gg R_i$). However, a large value of the droop coefficient will result in further deviation in the output voltage of the converters, and, consequently, lead to a further deterioration of the DC bus voltage. Also, a large droop gain has the potential of affecting the stability of the MG [12].

III. Proposed Droop Coefficient Design and Optimization

The objectives of the optimization are to minimize the error of the current sharing ratio between the paralleled converters in an islanded DC MG of MEA EPS and to achieve an acceptable regulation of the DC bus voltage.

A. Formulation of the Multiobjective Optimization (MOO) Problem

In this section, the multiple objective functions of the optimization problem are formulated. The GA is employed for searching the optimal droop coefficients within the design space. The optimal design will guarantee an accurate current sharing ratio between the converters and enhanced the DC bus voltage regulation. In this paper, three droop coefficients of the converters are considered the design variable in the optimization problem. The optimization problems are formulated as follows;

1) Improvement in Current sharing Ratio: In the optimization problem of a three-source MG system, the output DC current sharing ratio between the converters can be expressed as in (6) and (7). It is worth noting that the output current of converter 1 is used as the base value.

$$n_1 = \frac{I_{dc2}}{I_{dc1}} = \frac{k_{d1}+R_1}{k_{d2}+R_2} \tag{6}$$

$$n_2 = \frac{I_{dc3}}{I_{dc1}} = \frac{k_{d1}+R_1}{k_{d3}+R_3} \tag{7}$$

where n_1 and n_2 are the current sharing ratio between converter 1 and 2, and converter 1 and 3 respectively. The current sharing ratios will not be as desired due to the influence of the mismatched line resistance on the current sharing performance of the droop control method. However, for a desired equal current sharing among the converters, the current sharing ratios between the converters (i.e. $n_{1desired} = 1$, and $n_{2desired} = 1$) should be equal to 1. In other words, for equal current sharing among the converters, the absolute difference of the ith current sharing ratios between the converters from 1 should be equal to zero or as close to zero as possible. Therefore, the error in the current sharing ratio can be formulated as the first two objectives:

$$f_1 = \begin{cases} f_{1\_1} = |n_{1i} - 1| \\ f_{1\_2} = |n_{2i} - 1| \end{cases} \tag{8}$$

where f_{1_1} represents the error in the ith current sharing ratio between converters 1 and 2, f_{1_2} denotes the error in the ith current sharing ratio between converters 1 and 3.

2) DC Bus Voltage Regulation: The third objective is defined as the regulation of the DC bus voltage. The DC bus voltage should be regulated as close to the nominal value as possible and it should not go below 5% of the nominal value. The third objective (f_2) is formulated as the minimization of the error between the ith DC bus voltage (V_{bi}) and the desired system DC bus voltage ($V_{bdesired}$) for the considered maximum loading condition:

$$f_2 = |V_{bin} - V_{bdesiredn}| \tag{9}$$

$$V_{bin} = \frac{V_{bi}}{270} \tag{10}$$

$$V_{bdesiredn} = \frac{V_{bdesired}}{270} \tag{11}$$

where V_{bin} is the normalized ith DC bus voltage and $V_{bdesiredn}$ is the normalized desired DC bus voltage. The minimization of the formulation in (9) should return zero or a value close to zero for the desired control objective to be realized. Therefore, the optimization problem involves searching for the optimal droop coefficients $k_{dioptimal}$ that minimizes the overall system error functions formulated in (8) and (9). The overall system error function f_T can be expressed as in (12).

$$f_T = f_1 + f_2 = f_{1\_1} + f_{1\_2} + f_2 \tag{12}$$

To find the optimal design point that will yield the desired accurate current sharing ratio and acceptable DC bus voltage regulation, an integrated objective function d is formulated as expressed in (13).

$$d_i = \sqrt{\left(\frac{f_{1\_1i}}{f_{1\_1max}}\right)^2 + \left(\frac{f_{1\_2}i}{f_{1\_2max}}\right)^2 + \left(\frac{f_2 i}{f_{2max}}\right)^2} \tag{13}$$

The optimal design point can be obtained using the expression in (14).

$$[minimum, position] \equiv min\ (d_i) \tag{14}$$

3) Optimization Constraints: The multiobjective problem formulated in (8) and (9) are solved by subjecting them to some constraints as in (13)-(14). This is to ease the convergence of the optimization process to the optimal droop coefficient. The first constraint expressed in (13) is to ensure that the droop coefficients are computed within a certain design space that is reasonable and with high fidelity. Most importantly, the design space of the droop coefficients must be such that the system stability is not affected. Based on this, the lower and upper boundary of the droop coefficient is defined as -10% and +10% respectively of the conventional droop coefficient shown in Table I.

$$k_{di}^{\ lower} \leq k_{di} \leq k_{di}^{\ upper} \tag{13}$$

The second constraint to satisfy the desired bus voltage regulation is as expressed in (14).

$$V_0 - V_{bi} \leq \delta V_{max} \tag{14}$$

This constraint shows that the difference between the nominal DC bus voltage *(V_o)* and the *i*th DC bus voltage *(V_{bi})* should not exceed 5% of the nominal bus voltage value. Therefore, the MOO problem formulated in (8) and (9) and subjected to the constraints in (13) and (14) will be solved using the GA. The GA optimization procedure is discussed in the next subsection.

B. GA Optimization

The GA is one of the most popular metaheuristic techniques used in solving MOO problems [23]. It helps in picking out the Pareto optimal front solutions from the search space. The GA exist in various variants as can be found in [24], however, the controlled, elitist GA is used in this paper. It has been found that elitism can help significantly in enhancing the performance of the GA [24]. The GA deal with a system as a black box. It evaluates the fitness of each design point based on the output in the current generation and thereafter determines the new input in the next generation based on selection, crossover, and mutation operators [25, 26, 27]. In GA, a random search is carried out within a defined design space when solving an optimization problem.

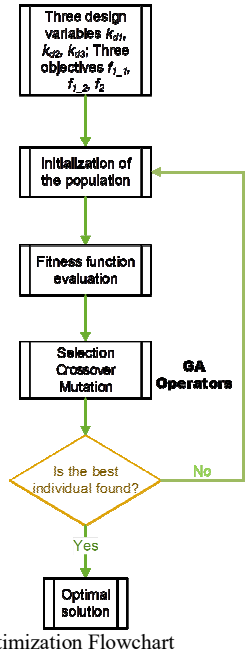

Fig. 4. GA Optimization Flowchart

There are three design variables for the three source system being considered in this paper and their design space is shown in Table II. The Pareto optimal front is obtained using the GA function from MATLAB's global optimization toolbox. Thereafter, an index function integrating the objective functions (13) is used to obtain the best design from the Pareto optimal front solutions. The optimization process and results obtained will be discussed in the following sub-subsections.

1) Optimization Variables, Constraints and System Parameters: The parameters of the system used as a case study, optimization constraints and system line parameters and the search range for the design variables are shown in TABLES I and II respectively. The GA MATLAB toolbox is used in this paper and the GA parameters such as the Pareto fraction, population size and the maximum number of generations are shown in TABLE I. The default setting of the other GA parameters was used. The results obtained at each iteration will be subjected to the constraints in (13) and (14). The potential solutions that meet these constraints will be considered the feasible design point.

TABLE I. PARAMETERS USED IN THE DESIGN AND OPTIMIZATION

	Parameters and Symbol	***Value***
System	Rated Voltage of main DC Bus V_o	270 V
	Local Shunt Capacitor C_i	1.2 mF
	Main DC bus capacitor C_b	0.6 mF
	Converter 1 conventional droop coefficient k_{d1}	1/4.25
	Converter 2 conventional droop coefficient k_{d2}	1/4.25
	Converter 3 conventional droop coefficient k_{d3}	1/4.25
	Line 1 Resistance R_1	3 mΩ
	Line 2 Resistance R_2	30 mΩ
	Line 3 Resistance R_3	15 mΩ
GA	Population size	100
	Maximum generation number	50
	Pareto fraction	0.3
Constraint	The maximum allowable DC bus voltage deviation is δV_{max}	5%

TABLE II. DESIGN SPACE FOR OPTIMIZATION

Variable	***Range***
k_{d1}	[1/3.825, 1/4.675]
k_{d3}	[1/3.825, 1/4.675]
k_{d3}	[1/3.825, 1/4.675]

2) Optimization process: Fig. 4 shows a flowchart of the steps involved in the proposed GA based optimization. In the first instance, the initialization of the population is executed by defining the variables for optimization. Each individual in the population represents a potential solution to the

optimization problem and is referred to as a chromosome. Consequently, many potential solutions are generated at random through successive iterations. These iterations are referred to as generations. By evaluating the fitness value (i.e. objectives of the optimization) of each chromosome, the better individual solution is selected. Furthermore, the potential solution is either merged (i.e. crossover) or modified (i.e mutation) and replaced with new potential solutions (i.e. next generation) at each iteration. This way, the quality of the population in the present generation is greatly enhanced. The process is repeated until the optimum or suboptimal solution to the optimization problem is approached or the maximum number of generation pre-set is attained.

3) Optimization results: The MOO was successfully implemented using the GA toolbox and some code in MATLAB version R2021b. With a population size of 100 and 50 generations, a total of 5000 design points were generated. Out of the 5000 design points, however, only 4857 design points are feasible because only these points satisfied the constraints conditions in (13) and (14). Furthermore, 30 design points constitute the Pareto front solutions of the current sharing ratio and DC bus voltage regulation of the MOO problem. The optimization was carried out using a maximum load demand of 40 kW. The distribution of the feasible design points obtained during the optimization for the objective functions (f_{1_1}, f_{1_2} *and* f_2) and the design variables (k_{d1}, k_{d2} *and* k_{d3}) are shown in Fig. 5 and 6 respectively.

For equal current sharing among the converters, the desired current sharing ratios between the converters are $n_{1desired} = 1$ and $n_{2desired} = 1$. Also, the DC bus voltage desired in this paper is chosen as 257 V (i.e. 0.9518 when normalized). The chosen bus voltage is within the optimization constraints and did not violate the MIL-STD 704F standard. The distribution of the error in the ith current sharing ratios (f_{1_1}, f_{1_2}) and bus voltage deviations (f_2) within the feasible design space is shown in Fig. 5. The distribution of the design variables (k_{d1}, k_{d2} and k_{d3}) that yield the corresponding error in current sharing ratio and bus voltage deviation is shown in Fig. 6.

a) Optimal result: The optimal design variable was obtained front the Pareto front with the aid of the integrating function in (13) and (14). As shown in (14), the integrating function finds the minimal distance from the ideal objectives while looking for the optimal design point. Therefore, the optimal design variables that yielded the desired control objectives are $k_{d1optimal} = 1/4.0096$, $k_{d2optimal} = 1/4.4961$ and $k_{d3optimal} = 1/4.2119$ as shown in Fig. 6.

IV. Simulation Studies

The performance of the conventional droop control method when using the conventional droop coefficients (in TABLE I) is compared with that of using the optimal droop coefficients. A CPL of 40 kW was applied at 0.2 s during the simulation. The simulation results of the validation and comparison for the desired equal sharing ratio (i.e. $n_{1desired} = 1$ and $n_{2desired} = 1$) and desired bus voltage regulation are shown in Fig. 7.

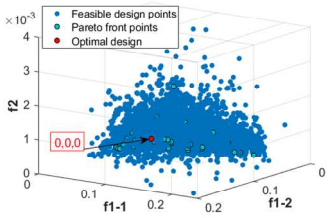

Fig. 5. Optimized Objective Functions distribution and the best design point

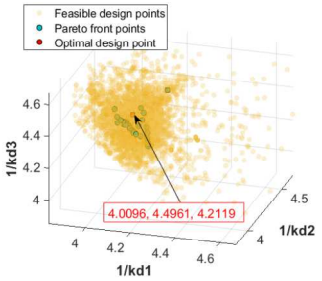

Fig. 6. Optimized Design variables distribution and the best design point

It can be seen from Fig. 7 (a) that the current sharing ratios between the converters in steady-state using the conventional fixed droop coefficients are $n_1 = 0.8983$ and $n_2 = 0.9520$ (with current sharing of $I_{dc1} = 54.610$ (A), $I_{dc2} = 49.056$ (A) and $I_{dc3} = 51.990$ (A)). The inaccurate current sharing ratio in the conventional droop control methods is due to the influence of unequal cable resistance. On the other hand, using the optimal droop coefficients, the desired equal sharing ratio between the converters of $n_{1desired} = 1$ and $n_{2desired} = 1$ is realized (with current sharing of $I_{dc1} = 51.90$ (A), $I_{dc2} = 51.90$ (A) and $I_{dc3} = 51.90$ (A)) as shown in Fig. 7 (b). Hence, the optimal droop coefficient combination can mitigate the influence of the corresponding subsystem's line resistances on accurate current sharing.

Also, the performance of the droop control method in terms of the DC bus voltage regulation when using the conventional fixed droop coefficient was compared to when using the fixed optimal droop coefficients as shown in Fig. 7 (a) and (b) respectively. It can be observed that in both scenarios, when a constant power load of 40 kW was applied to the system at 0.2 s, the main DC bus voltage dropped to 257 V (V_{bconv}) and 256.9 V (V_{prop}) from its initial value of 270 V due to the increase in the load current. Hence, the voltage regulation performance is similar and within the acceptable range.

V. Conclusions

The computation of the optimal droop coefficient of converters in the islanded DC MG of the MEA EPS distribution network using GA optimization is proposed in this paper. The minimization of the error in the current sharing ratio between the converters and the bus voltage regulation is considered the objective of the optimization. The GA was used to obtain the Pareto front solution to the MOO problem, thereafter a simple integrating objective function is used to extract the best design. Based on the results obtained, the fixed

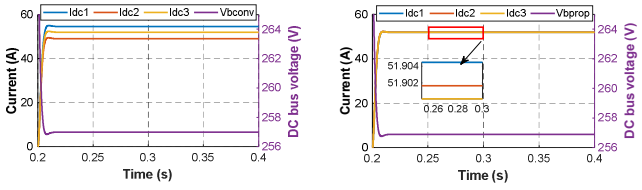

(a) (b)

Fig. 7. (a) Current sharing and bus voltage regulation using the conventional fixed droop coefficient (b) Current sharing and bus voltage regulation using the fixed optimal droop coefficient

optimal droop coefficient that is obtained using the proposed approach can improve the steady-state performance of the droop control method when compared to the conventional fixed droop coefficient.

ACKNOWLEDGMENT

This work has received funding from the Clean Sky 2 Joint Undertaking under the European Union's Horizon 2020 research and innovation programme under grant agreement No 807081. The author Habibu Hussaini extends his profound appreciation to the Petroleum Technology Development Fund (PTDF), Nigeria, for the scholarship funding.

REFERENCES

[1] J. A. Rosero, J. A. Ortega, E. Aldabas and L. A. R. L. Romeral, "Moving towards a more electric aircraft," *IEEE Aerospace and Electronic Systems Magazine,* vol. 22, no. 3, pp. 3-9, 2007.

[2] H. Hussaini, T. Yang, C. Wang and S. Bozhko, "An Enhanced and Cost Saving Droop Control Method for Improved Load Sharing for the MEA Application," in *2021 IEEE Transportation Electrification Conference & Expo (ITEC)*, Chicago, USA, 2021.

[3] F. Gao, S. Bozhko, A. Costabeber, G. Asher and P. Wheeler, "Control design and voltage stability analysis of a droop-controlled electrical power system for more electric aircraft," *IEEE Transactions on Industrial Electronics,* vol. 64, no. 12, pp. 9271-9281, 2017.

[4] J. P. Lopes, C. L. Moreira and A. G. Madureira, "Defining control strategies for microgrids islanded operation," *IEEE Transactions on power systems,* vol. 21, no. 2, pp. 916-924, 2006.

[5] M. A. Pedrasa and T. Spooner, "A survey of techniques used to control microgrid generation and storage during island operation," in *AUPEC2006*, 2006.

[6] R. A. Ferreira, H. A. Braga, A. A. Ferreira and P. G. Barbosa, "Analysis of voltage droop control method for dc microgrids with Simulink: Modelling and simulation," in *2012 10th IEEE/IAS International Conference on Industry Applications* , November, 2012.

[7] J. M. Guerrero, J. C. Vasquez, J. Matas, L. G. De Vicuña and M. Castilla, "Hierarchical control of droop-controlled AC and DC microgrids—A general approach toward standardization," *IEEE Transactions on industrial electronics,* vol. 58, no. 1, pp. 158-172, January 2011.

[8] J. M. Guerrero, M. Chandorkar, T. L. Lee and P. C. Loh, "Advanced control architectures for intelligent microgrids—Part I: Decentralized and hierarchical control," *IEEE Transactions on Industrial Electronics,* vol. 60, no. 4, pp. 1254-1262, April 2013.

[9] H. Hussaini, T. Yang, Y. Gao, C. Wang, M. A. A. Mohamed and S. Bozhko, "Artificial Neural Network Aided Cable Resistance Estimation in Droop-Controlled Islanded DC Microgrids," in *IECON 2021 – 47th Annual Conference of the IEEE Industrial Electronics Society*, Toronto, Canada, 2021.

[10] A. Tah and D. Das, " An enhanced droop control method for accurate load sharing and voltage improvement of isolated and interconnected DC microgrids," *IEEE Transactions on Sustainable Energy,* vol. 7, no. 3, pp. 1194-1204, 2016.

[11] Y. W. Li and C. N. Kao, "An accurate power control strategy for power-electronics-interfaced distributed generation units operating in a low-voltage multibus microgrid," *IEEE Transactions on Power Electronics,* vol. 24, no. 12, pp. 2977-2988, 2009.

[12] X. Lu, J. M. Guerrero, K. Sun and J. C. Vasquez, "An improved droop control method for dc microgrids based on low bandwidth communication with dc bus voltage restoration and enhanced current sharing accuracy," *IEEE Transactions on Power Electronics,* vol. 29, no. 4, pp. 1800-1812, 2014.

[13] V. Nasirian, A. Davoudi, F. L. Lewis and J. M. Guerrero, "Distributed adaptive droop control for DC distribution systems," *IEEE Transactions on Energy Conversion,* vol. 29, no. 4, pp. 944-956, 2014.

[14] F. Cingoz, A. Elrayyah and Y. Sozer, "Optimized droop control parameters for effective load sharing and voltage regulation in DC microgrids," *Electric Power Components and Systems,* vol. 43, no. 8-10, pp. 879-889, 2015.

[15] F. Cingoz, A. Elrayyah and Y. Sozer, "Optimized settings of droop parameters using stochastic load modeling for effective DC microgrids operation," *IEEE Transactions on Industry Applications,* vol. 53, no. 2, pp. 1358-1371, March-April 2017.

[16] Shivam and R. Dahiya, "Distributed control for DC microgrid based on optimized droop parameters," *IETE journal of research,* vol. 66, no. 2, pp. 192-203, 2018.

[17] M. Mokhtar, M. I. Marei and A. A. El-Sattar, "Improved current sharing techniques for DC microgrids," *Electric Power Components and Systems,* vol. 46, no. 7, pp. 757-767, 2018.

[18] M. A. Hassan and M. A. Abido, "Optimal design of microgrids in autonomous and grid-connected modes using particle swarm optimization," *IEEE Transactions on power electronics,* vol. 26, no. 3, pp. 755-769, March 2011.

[19] A. M. Dissanayake and N. C. Ekneligoda, "Multiobjective optimization of droop-controlled distributed generators in DC microgrids," *IEEE Transactions on Industrial Informatics,* vol. 16, no. 4, pp. 2423-2435, April 2020.

[20] T. Guillod, P. Papamanolis and J. W. Kolar, "Artificial neural network (ANN) based fast and accurate inductor modeling and design," *IEEE Open Journal of Power Electronics,* vol. 1, pp. 284-299., 2020.

[21] X. Lu, J. M. Guerrero, K. Sun and J. C. Vasquez, " An improved droop control method for dc microgrids based on low bandwidth communication with dc bus voltage restoration and enhanced current sharing accuracy," *IEEE Transactions on Power Electronic,* vol. 29, no. 4, pp. 1800-1812, April 2014.

[22] MIL-STD-704F, " Department of Defense Interface Standard. Aircraft Electric Power Characteristics," [Online]. Available: http://everyspec.com/MIL-STD/MIL-STD-0700-0799/MIL-STD-704F_1083/. [Accessed 8 August 2019].

[23] S. Zhao, F. Blaabjerg and H. Wang, "An overview of artificial intelligence applications for power electronics," *IEEE Transactions on Power Electronics,* vol. 36, no. 4, pp. 4633 - 4658, 2021.

[24] K. Deb, A. Pratap, S. Agarwal and T. Meyarivan, "A fast and elitist multiobjective genetic algorithm: NSGA-II," *IEEE transactions on evolutionary computation,* vol. 6, no. 2, pp. 182-197, 2002.

[25] Y. Gao, T. Yang, S. Bozhko, P. Wheeler and T. Dragičević, "Filter design and optimization of electromechanical actuation systems using search and surrogate algorithms for more-electric aircraft applications," *IEEE Transactions on Transportation Electrification,* vol. 6, no. 4, pp. 1434-1447, 2020.

[26] Y. Gao, T. Yang, T. Dragičević, S. Bozhko, P. Wheeler and C. Zheng, "Optimal filter design for power converters regulated by FCS-MPC in the MEA," *IEEE Transactions on Power Electronics,* vol. 36, no. 3, pp. 3258-3268, March 2021.

[27] K. S. Tang, K. F. Man, S. Kwong and Z. F. Liu, "Design and optimization of IIR filter structure using hierarchical genetic algorithms," *IEEE Transactions on Industrial Electronics,* vol. 45, no. 3, pp. 481-487, 1998.